Ultrasonics - Sonochemistry 43 (2018) 114–119

Contents lists available at ScienceDirect

Ultrasonics - Sonochemistry

journal homepage: www.elsevier.com/locate/ultson

Controlled positioning of microbubbles and induced cavitation using a dual-frequency transducer and microfiber adhesion techniques

Alex H. Wrede[a], Aarthy Shah[a], Marilyn C. McNamara[a], Reza Montazami[a,b], Nicole N. Hashemi[a,b,*]

[a] Department of Mechanical Engineering, Iowa State University, Ames, IA 50011, USA
[b] Center for Advanced Host Defense Immunobiotics and Translational Comparative Medicine, Iowa State University, Ames, IA 50011, USA

ARTICLE INFO

Keywords:
Cavitation
Microbubbles
Traumatic brain injuries
Microfibers

ABSTRACT

We report a study on two methods that enable spatial control and induced cavitation on targeted microbubbles (MBs). Cavitation is known to be present in many situations throughout nature. This phenomena has been proven to have the energy to erode alloys, like steel, in propellers and turbines. It is recently theorized that cavitation occurs inside the skull during a traumatic-brain injury (TBI) situation. Controlled cavitation methods could help better understand TBIs and explain how neurons respond at moments of trauma. Both of our approaches involve an ultrasonic transducer and bio-compatible Polycaprolactone (PCL) microfibers. These methods are reproducible as well as affordable, providing more control and efficiency compared to previous techniques found in literature. We specifically model three-dimensional spatial control of individual MBs using a 1.6 MHz transducer. Using a 100 kHz transducer, we also illustrate induced cavitation on an individual MB that is adhered to the surface of a PCL microfiber. The goal of future studies will involve characterization of neuronal response to cavitation and seek to unmask its linkage with TBIs.

1. Introduction

Cavitation refers to the spontaneous growth and collapse of MBs in low pressure regions. This process is currently used in a variety of areas, to mix fluids and eliminate impurities [1], as well as in specific drug delivery [2], gene therapy [3], and thrombolysis [4]. Previous research has also linked cavitation as a contributing factor in the exfoliation of graphene [5,6]. Additionally, cavitation has been shown to produce shock waves that have erosive effects on objects such as turbines and propellers [7–9]. Cavitation has also shown to produce a wide range of bioeffects. Previous studies sought out to identify cell damage that occurs in the midst of ultrasound therapy via calcium signaling processes [10]. On top of this, interested parties suspect that cavitation occurs inside the skull of TBI victims and its aftermath is leaving a profound impact [11–14]. Generation and characterization of controlled cavitation is critical to understand the cellular mechanisms of TBIs. These understandings can lead to better treatment that improves the quality of life for TBI victims, or it can even help launch preventative techniques that reduce the chance of a TBI altogether. In this study we use capillary tubing and an ultrasonic transducer to create two cost-effective methods for controlled cavitation. Our expectation is that these methods will be advantageous and applicable in future studies that focus on studying and understanding on the effects that cavitation has on nearby surfaces, like neurons in a TBI situation.

Acoustic cavitation occurs when the instantaneous pressure is negative, and a process of nucleation takes place [15]. Upon collapse of these MBs, micro jets form, localizing impact and force, causing damage to nearby surfaces [16]. This phenomenon is most visible in propellers, where the turbulent force of moving water creates areas of extreme low pressure, and over a period of time the blades experience significant erosion due to the repetitive impact of the cavitation shock waves [17]. There has been various techniques used in previous studies to study cavitation.

Acoustic, hydrodynamic, and optical methods have been implemented in previous studies to generate cavitation. In acoustic cavitation, ultrasonic waves are used to create cavitation, however previous methods do not have arbitrary control in the quantity of produced MBs and the specific location of their collapse is variant [18]. In hydrodynamic cavitation, fluid flows through an orifice, which increases the velocity and subsequently lowers threshold pressure so that nucleation occurs at the point of entry. With this method, vast amounts of MBs are generated, preventing the ability to analyze the effects of finite cavitation [19]. In optical induced cavitation, an intense energy is introduced to the system (laser), creating a stream of MBs in the beam of the laser. While this method is practical in creating controlled amounts of MBs, lasers are expensive and not accessible for a lot of research

* Corresponding author at: Department of Mechanical Engineering, Iowa State University, Ames, IA 50011, USA.
E-mail address: nastaran@iastate.edu (N.N. Hashemi).

https://doi.org/10.1016/j.ultsonch.2018.01.006
Received 7 December 2017; Received in revised form 4 January 2018; Accepted 4 January 2018
Available online 05 January 2018
1350-4177/

groups. Our approach is economical and offers a modification to the acoustic method to ultimately create a controlled environment to observe the effects of cavitation.

We introduced MBs into a water tank at a controlled size by pushing air through capillary tubing. We implemented two separate techniques to arbitrarily trap and position the MBs before induced cavitation. Our first method involves the use of a dual-frequency transducer [20]. The second method involves the MBs adhering to the surface of finely positioned PCL microfibers as they rise in solution. Using these techniques we were able to create, position, and collapse a finite number of MBs, as well as successfully illustrate live cavitation. These approaches are reproducible as well as affordable, providing more controlled and efficient techniques for cavitation studies.

2. Materials and methods

2.1. MB production

Capillary tubing with an inner diameter of 5 μm and an outer diameter of 360 μm (Molex, Lisle, IL), was used to produce the MBs. The tubing was attached to a 3 mL luer-lock syringe filled with air using a tubing adapter (Idex, Lake Forest, IL). A syringe pump (GenieTouch, Kent Scientific, Austin, TX) was used to plunge the syringe at a constant rate, allowing for the constant release of consistent sized MBs. The accuracy of all measurements were within ~2.7 μm due to the resolution of our imaging techniques. Sections 2.2 and 2.3 overview controlled cavitation via the dual-frequency method and via adhesion and resonant frequency, respectively. This orientation is followed throughout the Materials and Methods, Results, and Discussion sections.

2.2. Controlled MB positioning through a dual-frequency transducer

Fig. 1A represents the experimental setup for controlled MB positioning through the incorporation of a dual-frequency transducer. A 1.5 gallon tank filled with deionized water was used to house the existing components. This method was established through a developed study [20] which involves a point-focused, donut-shaped, (inner diameter of 14 mm and outer diameter of 30 mm, focal distance of 48 mm) ultrasound transducer with a center frequency of 1.6 MHz (ndtXducer, LLC, Northborough, MA). The transducer emitted brief ultrasound pulses to trap the MBs at the focus without collapsing them. The dual-frequency transducer is suspended in mid-solution through the attachment with a 3-axis adjustable stage (MT1, Thor Labs, Newton, New Jersey). This stage allows three-dimensional (3D) arbitrary movement of the transducers, which ultimately leads to 3D spatial control over MBs after they are trapped. PCL microfibers (Hashemi Lab, Iowa State University, Ames, IA) were placed above the capillary tubing and at the focal point of the transducer. There are three main reasons that the PCL microfibers were chosen to be used for this method. First, they have a delicate nature [21], allowing minimal disruption to the MBs and pressure field induced by the transducer upon entrapment. Second, they are used as a point of reference during the characterization of MB positioning. Lastly, these microfibers are known for their biocompatibility and potential in many future studies [22]. When not in simulation, the microfibers were preserved in ethanol to prevent infection and swelling. With the transducer focused at the level of the PCL microfibers and in line with the rising MBs, we were able to consistently trap and isolate individual MBs next to the PCL microfibers.

The central transducer induces oscillation on the MBs which ultimately leads to their collapse. The resonant frequency of a MB refers to the frequency at which it oscillates at a relative maximum amplitude [23]. When a MB oscillates with enough magnitude, it begins to fragment into smaller MBs, creating cavitation [24]. Eq. (1) represents the necessary calculation to find the resonant frequency of a MB with a known radius:

$$f_0 = 2\pi\sqrt{\frac{3\gamma P_0 + \frac{2\sigma}{R_0}}{\rho R_0^2} - \frac{2\sigma}{R_0}} \tag{1}$$

In this calculation, f_0 represents the first resonant frequency, R_0 designates the nominal bubble radius, ρ is the suspending mass density, γ denotes the gas phase polytropic constant, P_0 is the ambient pressure, and σ symbolizes the surface tension [25]. The size of the MBs generated through the capillary tubing ranged from 50 to 100 μm in diameter throughout our study. Plugging in the necessary parameters for Eq. (1), a MB with a 60 μm diameter will oscillate at a resonant frequency of ~100 kHz. We decided to use a 100 kHz transducer (diameter of 45 mm, unfocused) (Olympus, Waltham, MA) to achieve dramatic oscillation near the resonant frequency for 50–100 μm MBs. Since prior studies have shown the effectiveness of simultaneous dual-frequency functionality [20], it was ignored in this study. Our motivation is to demonstrate that a dual-frequency transducer would be effective through the combination of our positioning and cavitation results. The transducers were driven by a power amplifier (RAM-5000, Ritec, Warwick, RI). The magnified high-speed analysis was achieved by using

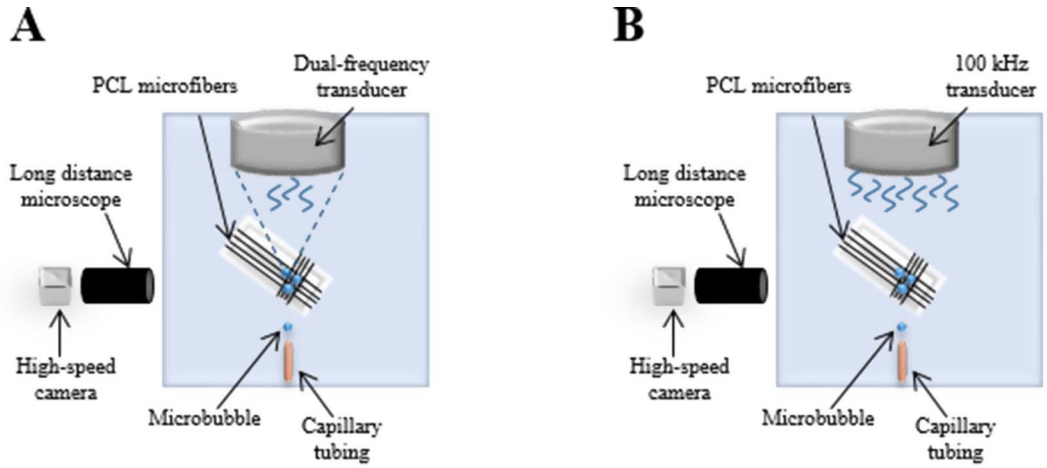

Fig. 1. (A) Apparatus for controlled MB positioning and collapse through using a dual-frequency transducer. The gap between the tip of the capillary tubing and the ultrasonic transducer was 70 mm. The gap between the PCL fibers and the ultrasonic transducer is 48 mm. The MBs are trapped at the focus of the 1.6 MHz outer-transducer (lowermost tip of the dotted lines). The 100 kHz central transducer is unfocused and is emitting sinusoidal waves. (B) Apparatus of controlled MB positioning and cavitation through adhesion and resonant frequency. The gap between the tip of the capillary tubing and the ultrasonic transducer is 70 mm. The gap between the PCL fibers and the transducer is 22.5 mm. The MBs are trapped through adhesion to the surface of the PCL microfibers.

a long distance microscope (Model K2, Infinity Photo-Optical Company) in unison with a high speed camera for imaging (BlackFly, FLIR).

2.3. Controlled MB positioning and collapse through adhesion and resonant frequency

The second method of controlled MB positioning and collapse is represented in Fig. 1B. PCL microfibers are also used in this approach and they are advantageous due to their ability to be adhesive to rising air bubbles. As the rising MBs came in contact with the PCL microfibers, they adhered to its surface. The PCL microfiber scaffold is suspended in mid-solution through the attachment with a 3-axis adjustable stage (MT1, Thor Labs, Newton, New Jersey). Three-dimensional control over the position of the scaffold allows for arbitrary control over the magnitude and position of trapped MBs. The transducer used in this approach is primarily to induce cavitation and has no influence on trapping and positioning of MBs. A 100 kHz transducer is also used in this method to accommodate resonant frequency conditions. The 100 kHz transducer is placed 22.5 mm (1/2 transducer diameter) above the PCL microfibers to maximize oscillation. The ultrasonic transducer was driven by a power amplifier (RAM-5000, Ritec, Warwick, RI). The high-speed analysis was achieved by using a long distance microscope (Model K2, Infinity Photo-Optical Company) in unison with a high speed camera for imaging (BlackFly, FLIR).

3. Results

3.1. MBs released from capillary tubing

Using different flow rates on the syringe pump, different sized bubbles can be generated. The rate at which MBs exit the capillary tubing can also vary. Fig. 2a shows MBs releasing from the capillary tubing at ~50 μm in diameter. This particular trial was operating with a flow rate of 100 μL/min on the syringe pump and they released from the capillary tubing at a rate of 50 MB/min. As the MBs increased in size, they required a greater pressure to collapse them. To create a greater pressure, the amplification of voltage to the transducer must also increase. Fig. 2b represents the necessary peak-to-peak voltage to fragment MBs with varying sizes. In other words, 100 kHz is approximately the resonant frequency of a 60 μm MB but it can induce cavitation on similar sized MBs if the operating voltage is varied. Varying the operating voltage also varies the acoustical pressure that is induced on the MBs.

3.2. MB positioning using dual-frequency method

Previous studies have shown that the impact of cavitation is most significant when the space between the MB and target material (D) is less than the diameter of the MB (d). The cavitation effects are greatly reduced when this ratio (D/d) increases [20]. Fig. 3 demonstrates the ability of the point-focused transducer to trap and suspend a MB in mid-solution through a pulsed signal (central frequency 1.6 MHz, 20 cycles, pulse repetition frequency 238 Hz, 250Vpp). Arbitrarily adjusting the 3-axis stage allowed for MB positioning toward the PCL microfiber. The MBs in Fig. 3 are moving at approximately 30 μm/s until they are held stationary when $D < d$. This was a typical speed for our trials because the MBs would often escape the focal region of the transducer if the adjustable stage was moved at a faster rate.

After the MBs were directed $D < d$ away from the target material, our apparatus also had arbitrary control over the vertical depth that the MBs resided in mid-solution. Fig. 4 shows the vertical dimension of the MB being adjusted as it remains $D < d$ away from the PCL microfiber (central frequency 1.6 MHz, 20 cycles, pulse repetition frequency 238 Hz, 250 Vpp). The MBs are less resistive to ascent in solution compared to movement in any other direction because of their buoyancy. The MBs represent this tendency in Fig. 4 as they rise around 75 μm/s.

3.3. MB positioning and collapse using microfiber adhesion and resonant frequency

Having complete control over the position of the PCL microfiber scaffold allowed for arbitrary control over the magnitude and position of trapped MBs. The scaffold is placed directly above the path of rising MBs and "catches" any MBs that come in contact with the PCL microfiber surface. After the MBs are trapped at desired locations, the scaffold is moved away from the rising MBs to eliminate any disturbance on the controlled environment. The 100 kHz transducer is then centered above the scaffold and used to induce cavitation (4 cycles, pulse repetition frequency 59 Hz, 100 Vpp). Fig. 5 captures this phenomena at high speed. After 16 ms the original MB is shown to fragment into three smaller MBs, illustrating cavitation.

4. Discussion

Although it is suspected that MBs form and collapse to create cavitation inside the skull during TBI situations [11], there is no direct research to understand the neuronal response to this phenomena. This

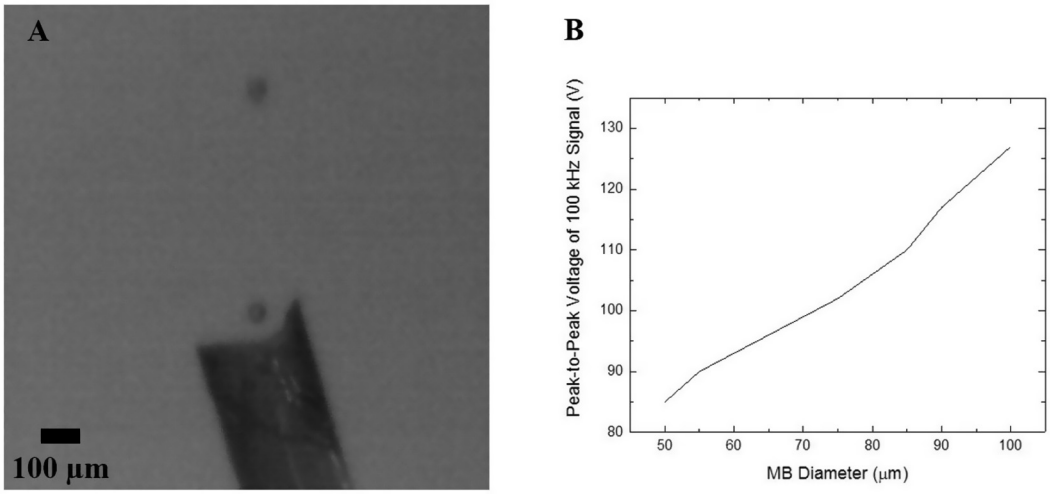

Fig. 2. (A) Air MBs releasing from capillary tubing. (B) Relationship between MB diameter and corresponding peak-to-peak voltage through the 100 kHz transducer that is necessary to collapse bubbles.

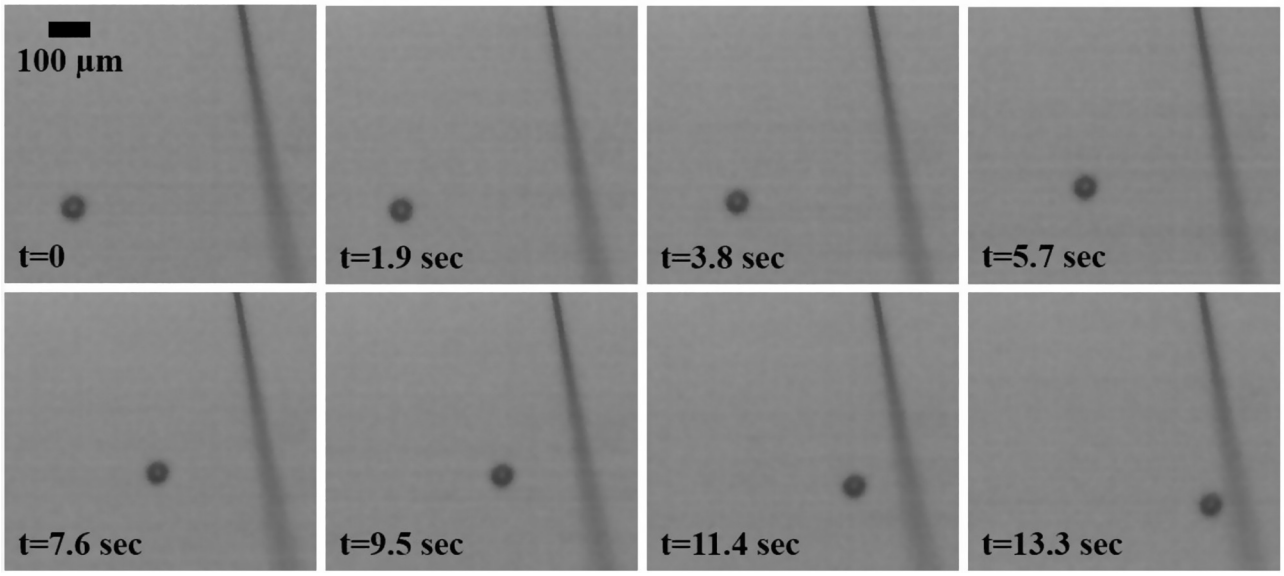

Fig. 3. Lateral MB positioning using the 1.6 MHz point-focused transducer.

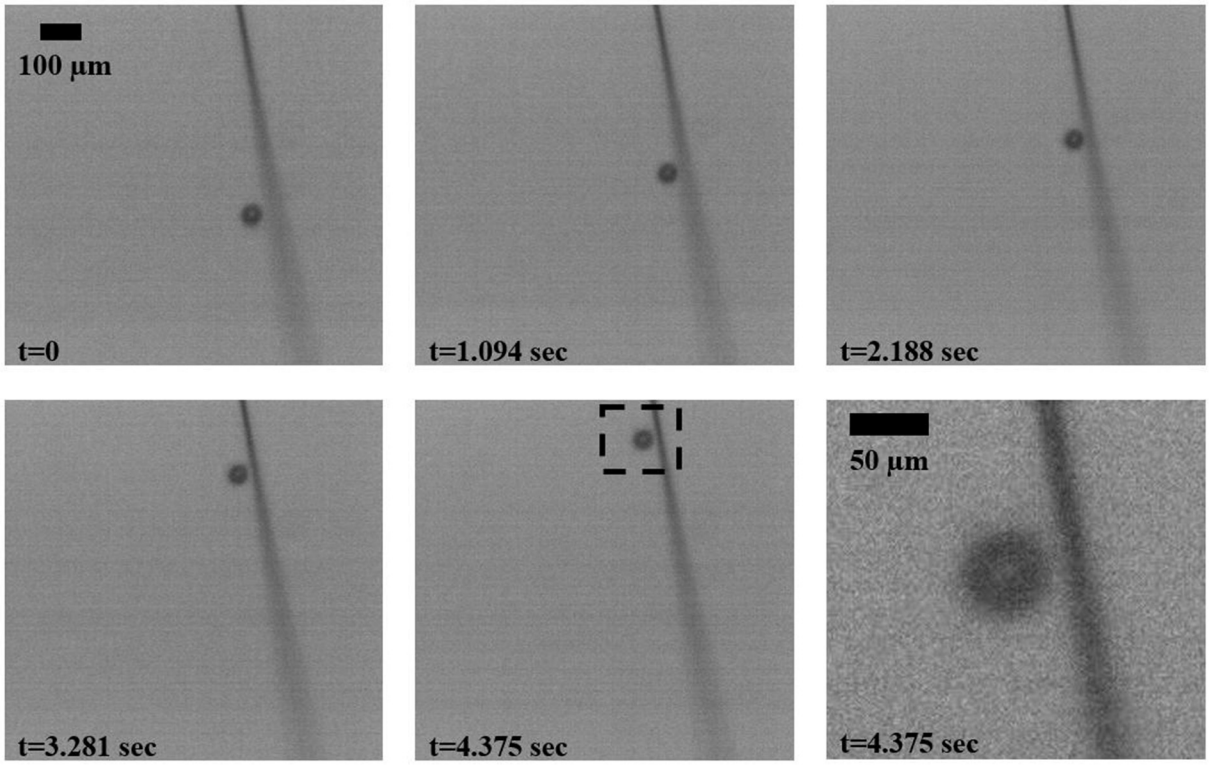

Fig. 4. Vertical MB positioning using the 1.6 MHz point-focused transducer. The final image is zoomed upon to show that the MB is clearly within one MB diameter length (d) from the PCL microfiber. It is estimated that at 4.375 s, the distance between the MB and the PCL microfiber is ~8 µm.

research could be the underlying building block that is used to answer questions about the nature of TBIs and the symptoms that they endow. Generating controlled cavitation is the first step to simulating these responses. Previous methods for the creation of cavitation are uncontrolled, and/or uneconomical. In this study, we developed a novel approach combining microfluidic and acoustical methods to create economical controlled cavitation. This approach offers intriguing potential for future studies to analyze the effects that cavitation has on surrounding materials. The PCL microfibers used in this study have been shown to successfully sustain living cells in previous research [22], which provides direct opportunity for bio-medical applications in future research.

4.1. MB production

We were able to generate MBs at a consistent rate, with the size of 50–100 µm. The generated MBs released from the tubing at a constant size throughout each trial but a given set of experimental parameters did not always produce the same size MBs from one trial to the next. This was not critical, though, because the size of the MBs remained within 50–100 µm, the range at which we hoped to produce for applications previously listed. Also, for our study it was more important to

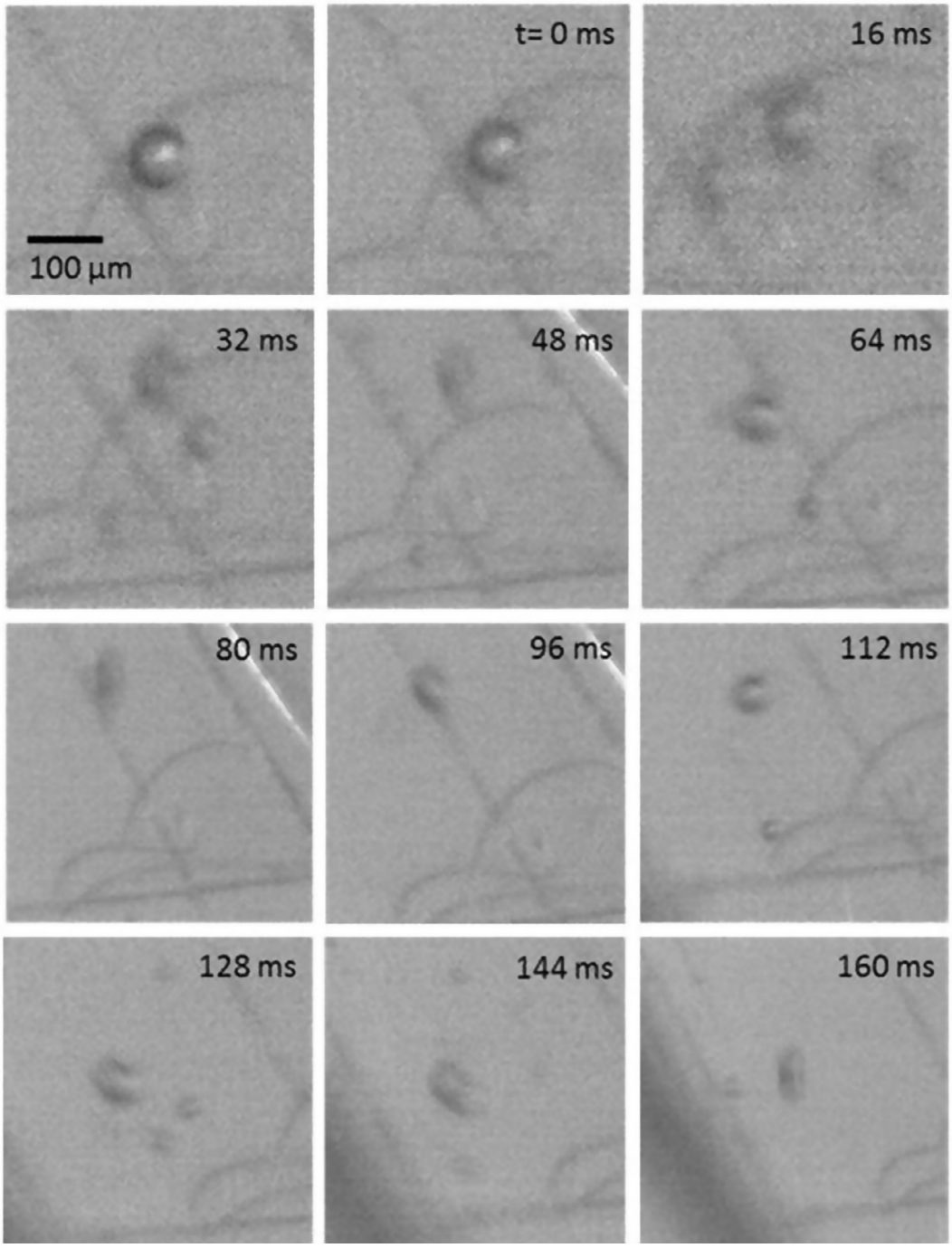

Fig. 5. Induced cavitation from the resonant frequency that the 100 kHz transducer provides. The images are captured at 62f/s. (See Supplemental Video 1).

get constant release of MBs with similar sizes than to have a narrow tolerance on the size variance from one trial to the next. A possible reason for the variability in size might be due to the erosion on the capillary tubing inside the luer-lock adapter. The pressure built up at this point is immense due to the difference in cross sectional area between the syringe and capillary tubing. We would occasionally recut the tubing to get rid of eroded material but the difference from one cut to the next is difficult to replicate on tubing with a 5 µm inner diameter and an outer diameter of 360 µm. A difference in the pattern of this cut likely changes the airflow inside the tubing and could be the underlying reason for variability in MB size. The rate at which the MBs exited the capillary tubing was also variant, likely due to similar reasons. This was not a critical issue in our study, as the 1.6 MHz was able to trap and isolate individual MBs regardless of their repetition rate. The rate at which they exited was also at a slow enough rate to "catch" arbitrary amounts of MBs with the PCL microfibers.

Using air as the gas that make up the MBs is advantageous when applying our project to a TBI situation. During a blast-induced TBI, MBs are expected to form inside the extracellular matrix which is concentrated with cerebrospinal fluid (CSF) that is primarily made up of water vapor, oxygen, and nitrogen [26]. Due to the similar chemical makeup of air, we decided its substitution in this project to realistically resemble a cavitation bubble from a blast-induced TBI is reliable.

4.2. MB positioning using dual-frequency method

An acoustical method for MB positioning was used in previous studies, which incorporated a dual-frequency transducer [20]. We extended on this approach by making future studies more advantageous for TBI studies. Previous research used optical methods to produce MBs which is often times uneconomical. We combined our MB production method (Section 2.1) with their acoustical methods to demonstrate 3D control over cavitation in a more economical manner. Using microfibers in our apparatus also allows for the study of a wide variety of cells in future studies. Previous methods have used voltage clamp electrodes to constrain cells but this is not feasible to maintain cell-viability for all types of cells. Our methods are advantageous to produce and have 3D control over MBs that are 50–100 μm, but if future works requires smaller MB size (~ 10 μm) then optical methods, similar to that of Zhou et al., would be more advantageous.

We ignored simultaneous positioning and cavitation through dual-frequency capability in this study but our combined results (Sections 3.2 and 3.3) demonstrate that a dual-frequency transducer with an outer frequency of 1.6 MHz and a central frequency of 100 kHz would be successful in doing so for future studies. This proven functionality provides direct opportunity to study the controlled effects that cavitation has on surrounding materials. Having the ability to arbitrarily control the spatial displacement between the MBs and target material (D) also provides opportunity to study the relationship between D and the target material response.

4.3. MB positioning and collapse using microfiber adhesion and resonant frequency

The methods and results shown in Sections 2.3 and 3.3 demonstrate encouraging capability that has potential to propel future studies. Due to the delicate nature of the PCL microfibers [27], future studies on cavitation characterization can be done. Our novel approach allows for the MBs to be trapped as they adhere to the surface of the microfibers. As cavitation occurs, the microfibers will have minimal disruption on its pattern, allowing for a detailed analysis on the stages of cavitation and its aftermath. The biocompatibility of the PCL microfibers will allow for the introduction of cell-laden microfibers [22], and ultimately will provide opportunity for future research on the effects of surface-cavitation and its consequences on surrounding cells. In regards to a TBI situation, using neuron-laden microfibers in our apparatus offers a realistic model that will mimic the consequences that surface-cavitation has on surrounding neurons. 3D control over the scaffold will allow for MB positioning and cavitation on arbitrary neurons.

5. Conclusions

In this study we have shown the success of MB production with a corresponding size of 50–100 μm. We have also demonstrated the success of two methods of controlled cavitation. These methods are cost-effective and provide arbitrary control on the position and magnitude of cavitation. These methods provide intriguing potential for future studies focused on the effects of cavitation on variable surfaces. In response to TBIs specifically, the two methods of controlled cavitation presented in this study provide an excellent opportunity to gather a detailed study on the neuronal response to cavitation. Future research that builds off of the techniques in this study involves using the biocompatibility of the PCL microfibers to seed neurons on its surface [22]. Using these neuron-laden microfibers in both of these methods will allow for characterization of neuronal response to cavitation and seek to unmask the unanswered questions in TBIs.

Acknowledgments

We thank Timothy Bigelow for his help with ultrasound logistics, Dan Barnard for his help with ultrasonic transducer, Travis Sippel for his help with imaging, and Hannah Rhoads. This work was partially supported by the Office of Naval Research (ONR) Grant N000141612246, ONR Grant N000141712620, U.S. Department of Energy Office of Science under the Science Undergraduate Laboratory Internship (SULI) Program at Ames Laboratory, and Iowa State University.

Appendix A. Supplementary data

Supplementary data associated with this article can be found, in the online version, at http://dx.doi.org/10.1016/j.ultsonch.2018.01.006.

References

[1] P.R. Gogate, A.M. Kabadi, A review of applications of cavitation in biochemical engineering/biotechnology, Biochem. Eng. J. 44 (2009) 60–72.
[2] C.M. Schoellhammer, G. Traverso, Low-frequency ultrasound for drug delivery in the gastrointestinal tract, Exp. Opin. Drug Delivery 13 (2016) 1045–1048.
[3] C.M.H. Newman, T. Bettinger, Gene therapy progress and prospects: ultrasound for gene transfer, Gene Ther. 14 (2007) 465–475.
[4] E.P. Stride, C.C. Coussios, Cavitation and contrast: the use of bubbles in ultrasound imaging and therapy, Inst. Mech. Eng. 224 (2) (2009) 171–191.
[5] Y. Gai, W. Wang, D. Xiao, Z. Yaping, Ultrasound coupled with supercritical carbon dioxide for exfoliation of graphene: simulation and experiment, Ultrason. Sonochem. 41 (2018) 181–188.
[6] R.K.L. Tan, S.P. Reeves, D.G. Thomas, E. Kavak, R. Montazami, N.N. Hashemi, Graphene as a flexible electrode: review of fabrication approaches, J. Mater. Chem. A 5 (2017) 17777–17803.
[7] A. Philipp, W. Lauterborn, Cavitation erosion by single laser-produced bubbles, J. Fluid Mech. 361 (1998) 75–116.
[8] L. Chernin, D.V. Val, Probabilistic prediction of cavitation on rotor blades of tidal stream turbines, Renewable Energy 113 (2017) 688–696.
[9] J. Bin, L. Xianwu, Y. Wu, Unsteady cavitation characteristics and alleviation of pressure fluctuations around marine propellers with different skew angles, J. Mech. Sci. Technol. 28 (2014) 1339–1348.
[10] F. Li, C. Yang, F. Yuan, D. Liao, T. Li, F. Guilak, P. Zhong, Dynamics and mechanisms of intracellular calcium waves elicited by tandem bubble-induced jetting flow, PNAS (2017), http://dx.doi.org/10.1073/pnas.1713905115.
[11] J. Goeller, A. Wardlaw, D. Treichler, J. O'Bruba, G. Weiss, Investigation of cavitation as a possible damage mechanism in blast-induced traumatic brain injury, J. Neurotrauma 29 (2012) 1970–1981.
[12] S. Canchi, K. Kelly, Y. Hong, M.A. King, G. Subhash, M. Sarntinoranont, Controlled single bubble cavitation collapse results in jet-induced injury in brain tissue, J. Mech. Behav. Biomed. Mater. 74 (2017) 261–273.
[13] R.S. Salzar, D. Treichler, A. Wardlaw, G. Weiss, J. Goeller, Experimental investigation of cavitation as a possible damage mechanism in blast-induced traumatic brain injury in post-mortem human subject heads, J. Neurotrauma 34 (2017) 1589–1602.
[14] C.M. Cartagena, et al., Subacute changes in cleavage processing of amyloid precursor protein and tau following penetrating traumatic brain injury, PLOS One 11 (2016).
[15] C.E. Brennen, Cavitation and Bubble Dynamics, Cambridge University Press, Cambridge, 2013.
[16] W. Lauterborn, C.-D. Ohl, Cavitation bubble dynamics, Ultrason. Sonochem. 4 (2) (1997) 65–75 1997/04/01.
[17] G. Kuiper, Cavitation research and ship propeller design, Appl. Sci. Res. 58 (1998) 33–50.
[18] M. Ashokkumar, The characterization of acoustic cavitation bubbles – an overview, Ultrason. Sonochem. 18 (4) (2011) 864–872 2011/07/01.
[19] P.R. Gogate, A.B. Pandit, A review and assessment of hydrodynamic cavitation as a technology for the future, Ultrason. Sonochem. 12 (1) (2005) 21–27 2005/01/01.
[20] Y. Zhou, K. Yang, J. Cui, J.Y. Ye, C.X. Deng, Controlled permeation of cell membrane by single bubble acoustic cavitation, J. Control. Release 157 (1) (2012) 103–111.
[21] Z. Bai, J.M.M. Reyes, R. Montazami, N. Hashemi, On-chip development of hydrogel microfibers from round to square/ribbon shape, J. Mater. Chem. A 2 (2014) 4878–4884.
[22] F. Sharifi, B.B. Patel, A.K. Dzuilko, R. Montazami, D.S. Sakaguchi, N. Hashemi, Polycaprolactone microfibrous scaffolds to navigate neural stem cells, Biomacromolecules 17 (2016) 3287–3297.
[23] D.B. Khismatullin, Resonance frequency of microbubbles: Effect of viscosity, J. Acoust. Soc. Am. 116 (2004) 1463–1473.
[24] M. Postema, A. Van Wamel, C. Lancee, N. De Jong, Ultrasound-induced encapsulated microbubble phenomena, Ultrasound Med. Biol. 30 (2004) 827–840.
[25] J.C. Buckey, D.A. Knaus, D.L. Alvarenga, M.A. Kenton, P.J. Magari, Dual-frequency ultrasound for detecting and sizing bubbles, Acta Astronautica 56 (9) (2005) 1041–1047 2005/05/01.
[26] S. Haniff, P.A. Taylor, In silico investigation of blast-induced intracranial fluid cavitation as it potentially leads to traumatic brain injury, Shock Waves 27 (2017) 929–945.
[27] F. Sharifi, D. Kurteshi, N. Hashemi, Designing highly structured polycaprolactone fibers using microfluidics, J. Mech. Behav. Biomed. Mater. 61 (2016) 530–540.